Iranian Journal of Physics Research, Vol. 18, No. 3, 2018

Research note

Measurement and simulation of magnetic field strenght in the nano magnetic abrasive finishing process

M Vahdati and A R Rasouli
Department of Mechanical Engineering, K.N. Toosi University of Technology, Tehran, Iran

E-mail: vahdati@kntu.ac.ir

(Received 16 August 2016 ; in final form 02 December 2017)

Abstract
Magnetic abrasive finishing can be classified as a non-traditional super finishing method for finishing surfaces with different shapes and working materials like flat plates, shafts, bearings parts, screws, tubes and many other mechanical parts that need good surface finishing properties. MAF is effective in polishing, cleaning, deburring and burnishing metal parts. The most important parameter affecting the performance of this method, such as surface roughness, is the magnetic force. The magnetic force is obtained from a permanent Magnet or a DC magnet. In this article, the magnetic field strength, magnetic flux density and magnetic force in different states are studied using simulation with some finite element method software (Maxwell). The shapes of magnets, various sizes and the material of fixture are studied. The magnetic properties of the material of the work piece are simulated too. To verify the simulation results, the situation is also measured by a Gauss meter. The intensity of the magnetic field required for the micro chipping is obtained for different geometric shapes and various materials of work piece in the magnetic abrasive finishing process. The results show that increasing the distance from the magnet surface results in a decrease in the magnetic flux density and significance of the edge phenomenon effect. The effect of work piece material, work piece fixture material, and the interaction of them were is shown to be significant on magnetic flux density. To concentrate the magnetic abrasive powder in the polishing process of non-ferromagnetic parts, the ferromagnetic fixture for these parts can be provided.

Keywords: magnetic abrasive finishing, design of experiments, simulation, magnetic flow density, teslameter

1. Introduction

It is necessary to obtain well-finished surfaces in high-tech industries such as aerospace, die polishing, and medicine. In applying conventional grinding and polishing techniques, there are some difficulties in finishing some advanced engineering materials or parts with complex shapes that should have high accuracy and minimal surface defects such as micro-cracks. New advanced finishing processes have been developed in last few decades to overcome limitations of the traditional finishing processes in terms of higher tool hardness requirement and precise control of the finishing forces [1]. This contributed to finishing harder materials and better process control over the final surface characteristics. Another limitation removed by some advanced finishing processes which use loose abrasives is the ability to finish complicated geometries by enhancing the availability of abrasive particles to the difficult-to-access regions of the work piece surface [2].

All these processes use multipoint cutting edges in the form of abrasives used to perform the cutting action. Higher hardness of abrasive particles is an important prerequisite for processing. If properly conducted, these abrasive machining processes can produce a surface of higher quality with a controlled surface roughness combined with a desirable residual stress distribution and freedom from surface and sub-surface damages.

On the basis of the energy used, the advanced finishing processes can be broadly categorized into mechanical, thermoelectric, electrochemical and chemical processes [3]. The performance and use of certain specific processes depend on work piece material properties and functional requirements of the component. In applying mechanical energy, very precise control over the finishing forces is required. Many newly developed processes make use of the magnetic/electric field to externally control the finishing forces on the abrasive particles. The magnetic abrasive finishing (MAF) process is a nano finishing

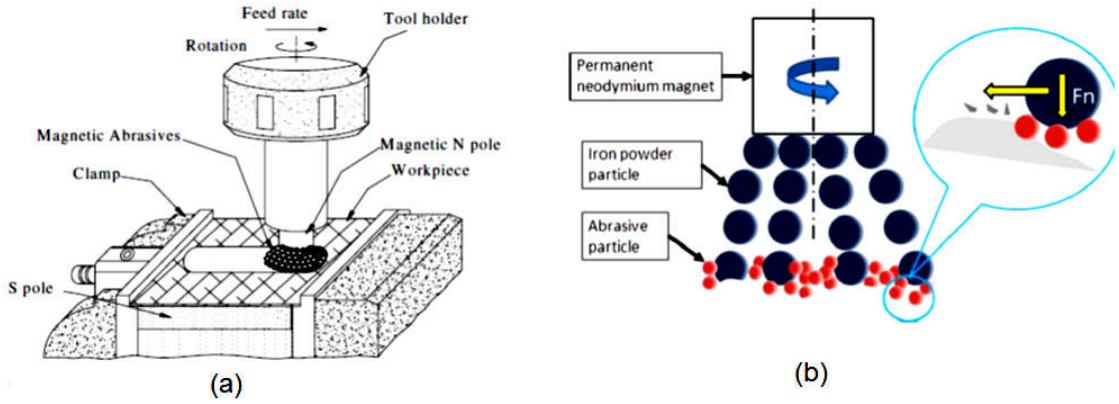

Figure 1. (color onlin) Magnetic abrasive finishing with the permanent magnet and the magnetic abrasive powder.

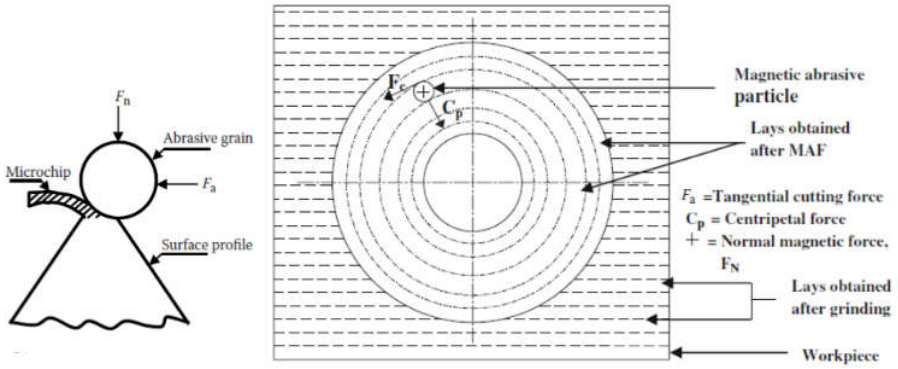

Figure 2. Schematic of the forces acting on MAF.

technique that can be employed to produce optical, mechanical, and electronic components with micrometer or sub-micrometer form accuracy and surface roughness within nanometer. This method was originally introduced in the Soviet Union, with further basic fundamental research in Japan, the United States, and India.

Regarding the importance of the magnetic field in the process of MAF and its effect on the quality of surface, in this paper, according to the form and size of the permanent magnet, work piece material (ferromagnetic, non-ferromagnetic), quality of the work piece fixture, and quality of the magnet fixture, the measurement and simulation of the magnetic flux density are considered to investigate the magnetic field strength exerted on the abrasive particles.

2. Magnetic abrasive finishing (MAF)

2.1. Fundamental principle

In MAF, magnetic forces play a dominant role in the formation of a flexible magnetic abrasive brush (FMAB), enabling abrasives to polish the work piece surface. Figure 1 (a) shows the working principle of the MAF of the plane surfaces [4]. MAF involves using a permanent or electronic magnet to generate a magnetic field in which magnetic abrasives are formed as a flexible magnetic brush for pressing and finishing a work piece. A mixture of abrasive and ferromagnetic powder forms the polishing tool called the FMAB. This magnetic abrasive powder fills the gap between the bottom face of the magnet and the top face of the work piece (Figure 1 (b). The ferromagnetic particles (magnetic iron powder) get aligned along the magnetic lines of force and form a chain-like structure known as a flexible magnetic abrasive brush. The abrasive particles (nonmagnetic in nature) get entangled within and between these chains. As the bond of the magnetic medium is soft and flexible, it can easily adapt to any non-uniformity in the shape of the surface being finished.

As shown in figure 2, two forces act on an abrasive particle. Normal force (F_n) is responsible for the penetration of the abrasive particle to the work piece surface, and axial force (F_a) removes the material in the form of microchips. In the plate MAF case, the relative motion between the FMAB and work piece, is provided by the rotation of the FMAB as well as the linear movement of the poles in the X-direction. As a result of the interaction between the fine abrasive grains and the work piece, the peaks of the work piece surface are sheared off by the rotation of the FMAB [5]. A limited amount of material will be removed by conducting a relative motion between the work piece surface and the abrasives so as to obtain a mirror-like finished surface.
Abrasive particles used in MAF are of different sizes and materials, such as silicon carbide (SiC) or alumina (Al2O3), which come in contact with and then finish the part's surface[5].These particles can be used in the form

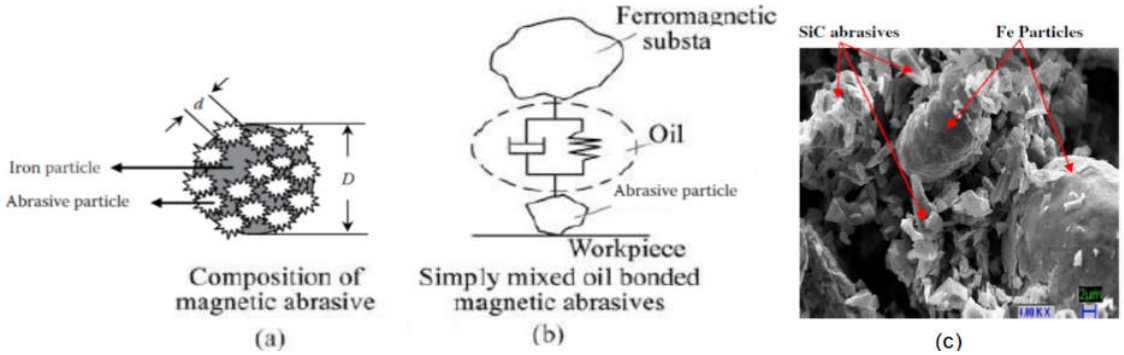

Figure 3. (color onlin) Schematic of (a)bonded, (b) unbonded magnetic abrasive particles, and (c) SEM micrograph of unbonded SiC abrasives (800 mesh).

of either bounded magnetic abrasive particles (BMAFs), in which abrasives are held in a ferromagnetic matrix, formed by sintering or other techniques, or they may be unbounded magnetic abrasive particles (UMAFs, a homogeneous mechanical mixture of ferromagnetic particles, abrasive particles, and additives). Figure 3 shows a schematic diagram of a micron-sized MAF (bonded (2 (a) unbonded (2 (b)). Wher D is the diameter of a single magnetic particle and d is the diameter of an abrasive particle held by an iron particle. Figure 3 (c) shows the SEM micrograph of the unbonded SiC abrasives of the 800 mesh number.

Furthermore, the disturbances from the base due to vibration or chatter will not affect the quality of the finished surface. MAF process offers many advantages, such as self-sharpening, self-adaptability and controllability; the finishing tool requires neither compensation nor dressing [6].

Due to micro cutting operation, temperature on the surface of the work piece is increased . A very high increase in temperature may deteriorate the surface quality of the work piece, but in MAF the temperature produced can be in the range of 34–51°C, not affecting the surface integrity and the surface finish of the work piece [7].

One of the main advantages of MAF operation, as compared with the traditional fine finishing operations like grinding, honing or lapping, is minimizing the possibility of producing micro cracks on the surface of the work piece because the cutting force is primarily controlled by the magnetic field and the finishing tool is a flexible magnetic brush made from the magnetic abrasive powder, while the other traditional finishing processes employ a rigid tool that subjects the work piece to substantial normal stresses which may cause micro cracks, thereby resulting in the reduced strength and reliability of the machined part.

2. 2. Dispersion of magnetic force

The MAF process is based on the electromagnetic behavior of the magnetic particles. MAFs acquire magnetic polarization and join each other along the lines of the magnetic force under the influence of the magnetic field, forming an FMAB. Knowledge of the distribution of magnetic forces on the work piece surface is essential to determine the surface quality to be produced.

The generalized equations used to solve the magnetic effect of currents, charges and time varying electrical fields are given by Maxwell's equations [8], as described in equation (1):

$$\vec{\nabla}.\vec{E} = \frac{\rho}{\varepsilon_0}\ ,$$
$$\vec{\nabla}.\vec{B} = 0\ ,$$
$$\vec{\nabla}.\vec{E} = -\frac{\partial \vec{B}}{\partial t}\ , \qquad (1)$$
$$\vec{\nabla}.\vec{B} = \mu_0 \vec{J} + \mu_0 \varepsilon_0 \frac{\partial \vec{E}}{\partial t}\ ,$$

where ε_0 is the permittivity of vacuum (F/m), ρ is the charge density (A/m²), E is the electric field intensity (V/m), B is the magnetic flux density (T), J is the electric current density (A/m²), and μ_0 is the relative magnetic permeability in vacuum (Wb/(A-m)). Time independent magnetic field problems (magneto static problems) are preferably solved based on magnetic scalar potential formulation. This reduces Maxwell's equations for magneto static problems to equation (2)

$$\vec{\nabla}.\vec{B} = 0\ ,$$
$$\vec{\nabla}.\vec{B} = \mu_0 \vec{J}\ , \qquad (2)$$

The above field equations are supplemented by the constitutive relation that describes the behavior of electromagnetic materials. For problems considering the magnetic saturation of materials without permanent magnets, the constitutive relation for the magnetic fields is given by equation (3)

$$\vec{B} = \mu \vec{H}\ , \qquad (3)$$

So, from equations (2) and (3), equation (4) can be derived

$$\nabla.\vec{H} = 0 \qquad (4)$$

where μ is the magnetic permeability of the medium and H is the magnetic field strength. The ferromagnetic materials have the property to get magnetized when placed in an external magnetic field.

There is no current source in the finishing gap. This process is assumed to be steady; therefore, the intensity of magnetic field H can be expressed as a gradient of the magnetic scalar potential ϕ [9], as written in equation (5).

$$\vec{H} = -\nabla\varphi \qquad (5)$$

Using equation (4) and (5), we can write equation (6).

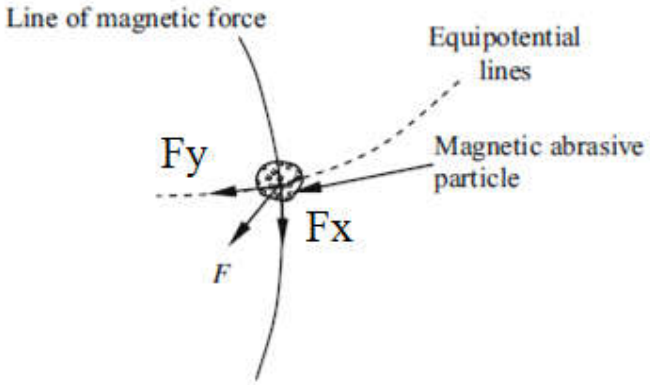

Figure 4. Enlarged view of the forces acting on magnetic abrasive particles.

$$-\nabla^2\varphi = 0 \quad . \tag{6}$$

On the basis of certain assumptions and consideration of the axisymmetric form of the problem, the governing equation of the process can be computed using equation (7).

$$\frac{1}{r}\frac{\partial}{\partial r}\left[r\mu_r\frac{\partial\varphi}{\partial r}\right]+\frac{\partial}{\partial z}\left[\mu_r\frac{\partial\varphi}{\partial z}\right]=0 \quad , \tag{7}$$

MAFs are composed of ferromagnetic and abrasive materials. The permeability of most ferromagnetic materials is not a constant value and varies with the field. This implies that equation (7) is nonlinear. The *r* and *z* components of the intensity of the magnetic field (H) are expressed as:

$$H_r = -\frac{\partial\varphi}{\partial r} \quad , \qquad H_z = -\frac{\partial\varphi}{\partial z} \quad , \tag{8}$$

Derivatives of H_r and H_z are evaluated using the Finite Difference (FD) method [10]. The obtained magnetic force exerted on the magnetic abrasive particle can be calculated in two ways. In both methods, magnetic field strength, as mentioned above, is required. As a d irect method into magnetic field, energy change occurs based on equations (9) and (10).

$$\vec{E} = -\frac{1}{2}\mu_0\vec{M}_C H \quad , \tag{9}$$

$$\vec{M}_C = \vec{M}.\vec{V} \quad , \qquad \vec{M} = \chi_r\vec{H} \quad , \tag{10}$$

In equation (10), $\vec{M}_C$ is magnetization and χ_r is the susceptibility of MAFs. The value of M from equation (10) is substituted in equation (9). Force acting on the sample in magnetic field with the gradient in direction *x* is according to equation (11) [11]

$$F = -\frac{dE}{dx} = \frac{1}{2}\mu_0 V\frac{d\left(M_C H\right)}{dx} = \mu_0\chi_m VH\frac{dH}{dx} \quad , \tag{11}$$

And resolving F into radial and axial directions, Equation (12) can be derived;

$$F_x = V\chi\mu_0 H\frac{\partial H}{\partial x} \qquad F_y = V\chi\mu_0 H\frac{\partial H}{\partial y} \quad , \tag{12}$$

Figure 4 shows that *x* is the direction of the line of magnetic force, *y* is the direction of the magnetic equipotential line, V is the volume of the magnetic particle, χ is the magnetic susceptibility of the particle, H is the magnetic field strength at point " i ", and $\partial H/\partial x$ and $\partial H/\partial y$ are the gradients of magnetic field strength in the x and y directions, respectively [12].

From equation. (12), the magnetic force F_x and F_y are proportional to the magnetic particle volume, susceptibility of the magnetic particle, the magnetic field strength and its gradients. The magnetic forces F_x and F_y are also capable of preventing the splashing of the magnetic abrasives, which could be due to the high speed rotation of the magnetic pole.

2. 3. Calculation of applied pressure on the work piece surface

During the finishing process, the congregated magnetic abrasives form a magnetic brush along the line of magnetic force within the working zone, causing the pressure *P* on the plane surface; this pressure will act on the abrasive particles based on equation (13)

$$P = \frac{B^2}{2\mu_0}\left(1-\frac{1}{\mu_m}\right), \qquad P = \left[\mu_0 H^2\left(1-\frac{1}{\mu_m}\right)\right]/2 \ , \tag{13}$$

where μ_m is the relative magnetic permeability of FMAB and can be expressed as equation (14) [13].

$$\mu_m = \frac{2+\mu_F-2(1-\mu_F)V_i}{2+\mu_F-(1-\mu_F)V_i} \ , \tag{14}$$

w here μ_F is the relative permeability of iron and V_i is the volume fraction of iron particles.

In the following, to calculate the exerted force on the abrasive particles, the exerted force can be multiplied by the cross-section surface (A); as a result, the total exerted force can be calculated using equation (15). In addition, regarding the high number of abrasive particles on the surface and the equality of the radius of particles, the number of particles can be calculated (n_a); in this way, the quantity of the exerted force for each particle can be obtained based on equation (16). In the second method, the location of the abrasive particles at the

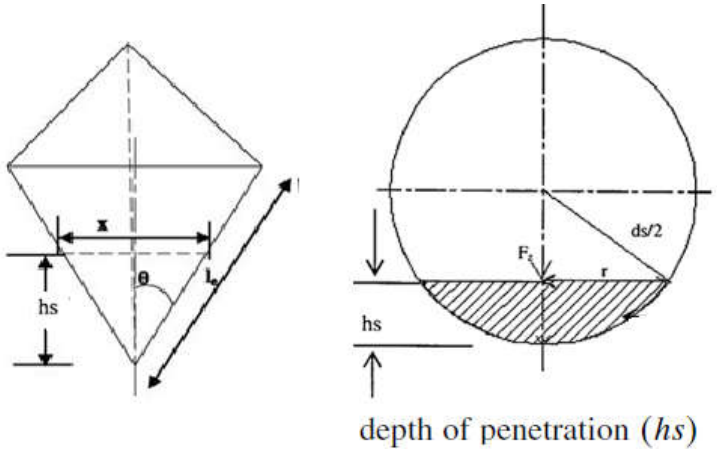

Figure 5. The amount of penetration into the work piece surface by the abrasive powder (a) spherical, and (b) tetrahedron.

surface of magnet is not effective, and a slight change occurs, except areas close to the edge of the magnet.

$$F_n = PA\,, \tag{14}$$

$$F_n = PA\,, \tag{15}$$

$$f_n = \frac{F_n}{n_a}\,, \tag{16}$$

3. Analysis of magnetic field strength

To analyze magnetic field strength, firstly, the effects of the magnetic force should be addressed. The most important effect of the magnetic force on magnetic particles is its influence on the surface of work piece or the so-called "jaggedness of surface". The magnetic particles apply the magnetic force to the abrasive particles. The depth of the penetration of abrasive particles on the surface of work piece, according to the structure of abrasive particles, is shown in figure 5.

The penetration depth is obtained from equations (17) and (18).

$$h_s = \frac{0.577}{\tan\theta}\sqrt{\frac{f_n}{H_d}}\,, \tag{17}$$

$$h_s = \frac{ds}{2} - \sqrt{\left(\frac{ds}{2}\right)^2 - \frac{F_n}{H_m \pi}}\,, \tag{18}$$

In figure 5 (a), the abrasive particle is spherical and in figure 5 (b), it is hexagon. h_s indicates the depth of the penetration of the abrasive particle on the surface of the work piece. In equations equations (17) and (18), F_n, h_s, θ and ds are the quantity of the magnetic force, the hardness of the workpiece, the angel of the abrasive particle, and the diameter of the abrasive particle, respectively. It is obtained from the relations that h_s depends on the magnetic force. If the quantity of magnetic force is excessive, it makes the brush of magnetic abrasive firm. The firmness of abrasive brush can reduce the quality of the surface of work piece and leave scratch on the surface. In addition, in cases where the smoothness of surface is necessary at the level of micron or nanometer, the penetration depth of abrasive particles must be at the same level or less. By selecting a too strong magnet or a short distance of gap, the magnetic force would be increased excessively, leaving scratch on the surface of the work piece. Furthermore, the excessive firmness of the abrasive brush causes abrasive particles not to have mobility when they are in contact with work piece and no change can be made in the quality of the surface over time and with the abrasion of the abrasive particles. On the other hand, if the magnetic force is extremely low, it will not have the capacity to retain magnetic abrasive particles at high velocity and makes the particles thrown. In addition to the magnetic field strength, the distribution way of the intensity of the field in the length of the magnet is extremely important. The behavior of the magnetic field toward ferromagnetic and non-ferromagnetic parts is also different.

Permanent magnets stimulations have been done in some past studies, but the dimensions of magnets and the material selection of parts and magnets fixture have not been studied in the measurement done by teslameter and also, in stimulations. Since we are looking for a micro and nano smooth surface, and we should consider the limited penetration of abrasive particles (in micro range), the importance of studying the effect of magnetic force on particles is highlighted.

Creating magnetic field strength is possible through electric and permanent magnets. Electric magnet within the boundary of the density of a magnetic field higher than 0.1 tesla occupies a large space. Moreover, in respect to the current flowing winders over time, the heat in the electric magnet increases considerably, requiring cooling equipment. Concerning the mentioned defects as well as the easier accessibility and the lower price of permanent magnet, the simulation and measurement of permanent magnets are analyzed. In figure 6, the electric magnet with its equipment is shown [4].

Permanent magnetic materials having energy products in excess of about 80 kJ/m^3 (10 MGOe) are considered to be of the high-energy type [3]. These are recently developed intermetallic compounds that have a variety of compositions; the two ones that have found commercial exploitation are SmCo5 and Nd2Fe14B.

Table 1. Properties of magnetic material

Material	Composition (wt %)	Remanence B_r [tesla (gauss)]	Coercivity H_c [amp-turn/m (Oe)]	$(BH)_{max}$ [kJ/m^3 (MGOe)]	Curie Temperature T_c [°C(°F)]	Resistivity ρ (Ω-m)
Tungsten Steel	92.8 Fe 6W, 0.5 Cr, 0.7C	0.95 (9500)	5900 (74)	2.6 (0.33)	760 (1400)	3.0×10^{-7}
Cunife	20Fe, 20 Ni, 60Cu	0.54 (5400)	44000 (550)	12 (1.5)	410 (770)	1.8×10^{-7}
Sintered alnice8	34Fe, 7Al, 15Ni, 35 Co, 4Cu, 5 Ti	0.76 (7600)	125000 (1550)	36 (4.5)	860 (1580)	
Sintered ferrite3	$BaO\text{-}6Fe_2O_3$	0.32 (3200)	240000 (3000)	20 (2.5)	450 (840)	$\sim10^4$
Cobalt rare earth1	$SmCo_5$	0.92 (9200)	720000 (9000)	170 (21)	725 (1340)	5.0×10^{-7}
Sintered Neodymium -iron-born	$Nd_2Fe_{14}B$	1.16 (11600)	848000 (10600)	255 (32)	310 (590)	1.6×10^{-6}

Table 2. Magnetic properties of Nd-Fe-B magnet.

Characteristics grade	Residual induction B_r	Coercive force bH_c	Intrinsic coercive force iH_c	Max. energy product (BH) max
N35	T kGs	kA/m kOe	KA/m kOe	KJ/m^3 MGOe
	1.17-1.21 11.7-12	860 10.8-11.4	≥ 95 ≥ 12.0	263- 279 33-35

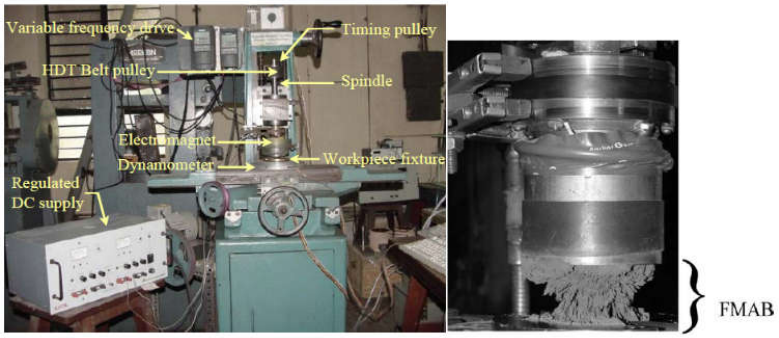

Figure 6. (color onlin) Electrical magnet with the equipment.

Samarium is a rare and relatively expensive material; furthermore, the price of cobalt is variable and its sources are unreliable. Consequently, the Nd2Fe14B alloys have become the materials of choice for a large number of applications requiring hard magnetic materials. Coercivities and energy products of these materials rival those of the samarium–cobalt alloys (table 1). These high-energy hard magnetic materials are employed in a host of different devices and in a variety of technological fields. One common application is in motors.

Permanent magnets are far superior to electromagnets in that their magnetic fields are continuously maintained without the necessity of expending electrical power; furthermore, no heat is generated during operation. Motors using permanent magnets are much smaller than their electromagnet counterparts, and they are utilized extensively in fractional horsepower units. Familiar motor applications include the following: in cordless drills and screw drivers; in automobiles (starting, window winder, wiper, washer, and fan motors); in audio and video recorders; and in clocks.

Temperature in the process of MAF does not increase considerably. For this reason, permanent magnets, which have high curie temperature, are not needed. According to the mentioned conditions, NdFeB (N35) was used to simulate and measure among the permanent magnets. The simulation was performed using the Maxwell finite element. In addition, tesla-meter (gauss-meter) was used to measure the density of the magnetic field.

3. 1. Analysis of geometric dimensions of the permanent magnets

The specifications of the N35 permanent magnet are presented in table 2. In the process of MAF on flat surfaces, since magnet has a rotational movement, a magnet with cylindrical geometry was used. The diameter and height of the magnet and the number of the used magnets are simulated in two-dimensional and three-dimensional modes. Simulation was performed using the Maxwell software package. Every type of Nd35 magnet with 1.3 T had the same density of nominal magnetic field, while output energy was different, depending on the geometrical conditions and the distance from magnet. Therefore, studying the

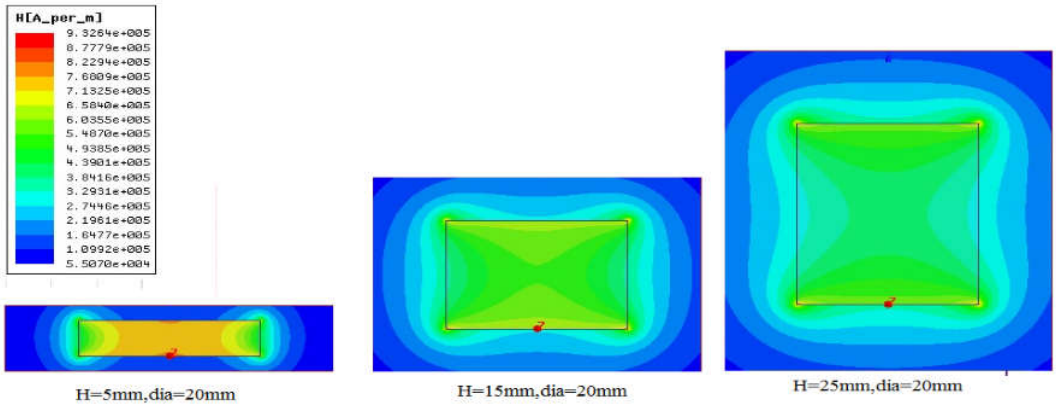

Figure 7. (color onlin) Magnetic field strength in different heights (dia, 20mm).

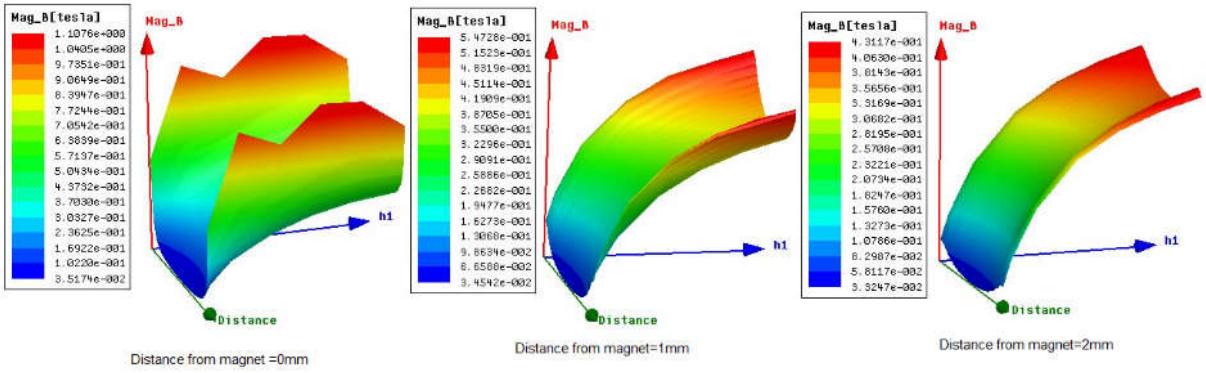

Figure 8. (color onlin) Magnetic flux density in different heights, on the surface and at 1 and 2 mm distance from the magnet.

quantities and behavior o the f magnet in different sizes and adjacency conditions is extremely important to analyze the magnetic force exerted on magnetic abrasive particles. Prominent differences between conventional and new MAF processes include the difference in the force imposed on the particles. This force is about some micro Newton; therefore, it causes a very small penetration depth into the work piece surface.

3. 1. 1. Analysis of the height of the permanent magnet

N35 permanent magnet with the diameter of 20 mm and the height of 5, 10, 15, 20 and 25 mm was simulated in 2D. figure 7 shows the magnetic flux density in different heights. In figure 8, with 3D Plots, the changes of magnetic flux density and magnetic field strength are shown in different heights and in different distances from the surface of magnet.

According to the diagrams, it could be observed that in a fixed diameter, with the increase in the height of the magnet, magnetic field intensity and magnetic flux density were increased. The significant difference in the quantities of the edges of magnet with those of other areas could be due to the effect of edge occurring in the magnet edges, and it was reduced in higher distances from the surface of magnet. This could be due to the fact that there were sharp edges/irregularities and sharp corners resulting in lower surface area, which increased the number of flux lines per unit area to pass through. This phenomenon is called edge/corner effect.

A number of experiments were performed in order to confirm the simulation and analysis of the effect of the height of cylindrical magnets. It is important to note that the measurement was performed by tesla-meter (PHVWE) on the surface of magnet, at the distances of 1 and 2 mm from the surface of magnet and in three points. All equipment used in the measurement of the magnetic flux density of the permanent magnet were made from non-ferromagnetic materials (figure 9).

In figure 10, the magnetic flux distribution graph obtained from simulation is presented in different distances on the 20 mm surface. Measured values by the gauss meter in a 2 mm distance from magnets of a 20 mm diameter and of 5 mm and 20 mm heights are presented in figure 11. Mean measured and simulated values at different distances from the surface of the fixture and magnet are reported in table 3. As can be seen, the changes in simulated and measured graphs were correlated with each other, and the differences between these values had a minimum of 4% and a maximum of 14%, while the simulated values were bigger than the measured ones.

3. 1. 2. Analysis of the diameter of permanent magnet

The height of the simulated magnet was 20 mm. The Diagrams 12 and 13 shos the change of the magnetic flux density and the magnetic field strength on the surface with the distance of 1 and 2 mm from the surface of the magnet. Permanent magnet with the diameter of10mm will have the highest magnetic flux density and magnetic field strength.

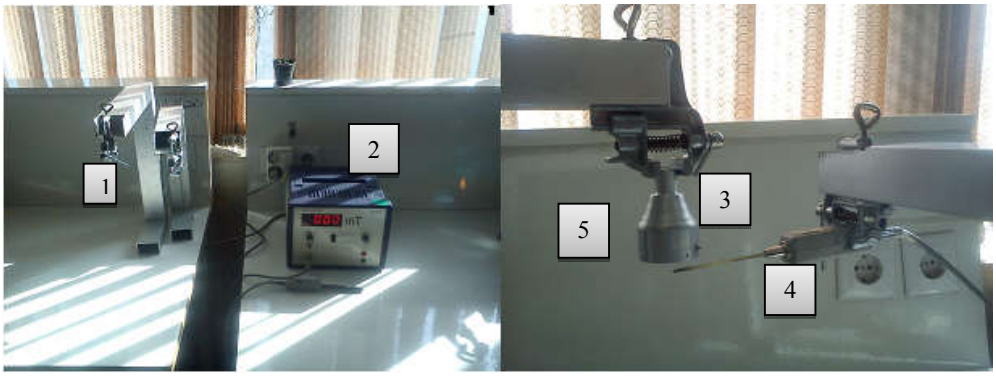

Figure 9. (color onlin) Measurement equipment (1) Aluminum stands, (2) phvwe teslameter device with a probe, (3) aluminum hook, (4) measurement probe, and (5) magnet aluminum fixture.

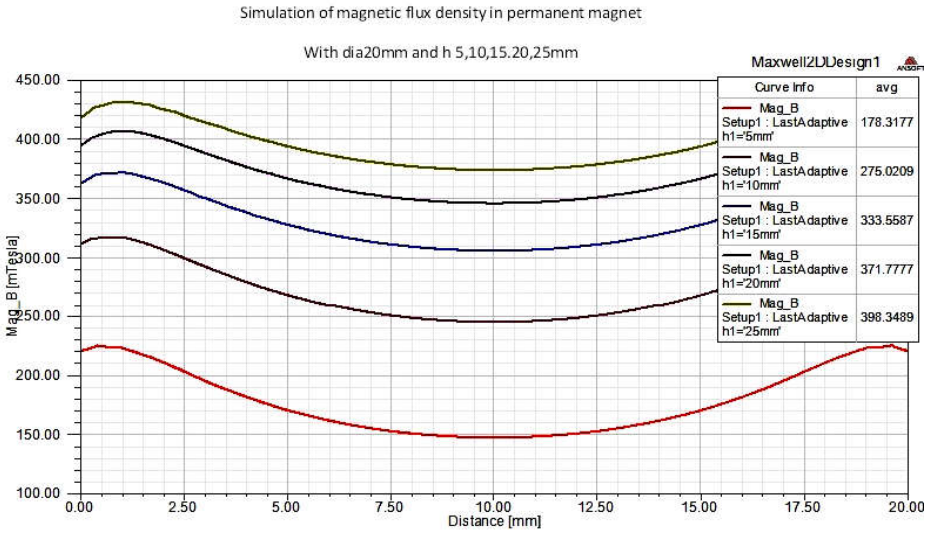

Figure 10. (color onlin) Magnetic flux distribution (militesla) in a magnet of 20 mm height and different heights in a 2 mm distance from the surface (simulated).

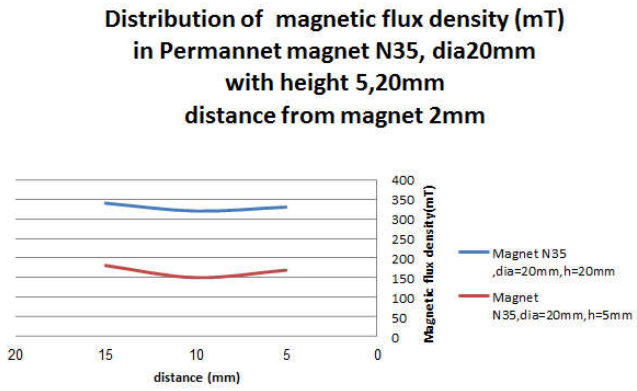

Figure 11. (color onlin) Magnetic flux distribution (militesla) in a magnet of 20 mm height and different heights in a 2 mm distance from the surface (measured).

Table 3. Average values of the measured and simulated Magnetic flux (militesla) in different distances from the magnet.

	N35,20mmΦ, 5mmheight Simulation (average)	N35,20mmΦ, 5mmheight Experimental (average)	N35,20mmΦ, 20mmheight Simulation (average)	N35,20mmΦ, 20mmheight Simulation (average)
Gap=0	264.1	243.33	503	443
Gap=1mm	208	200	422.9	371
Gap=2mm	178.3178	166.66	371	340

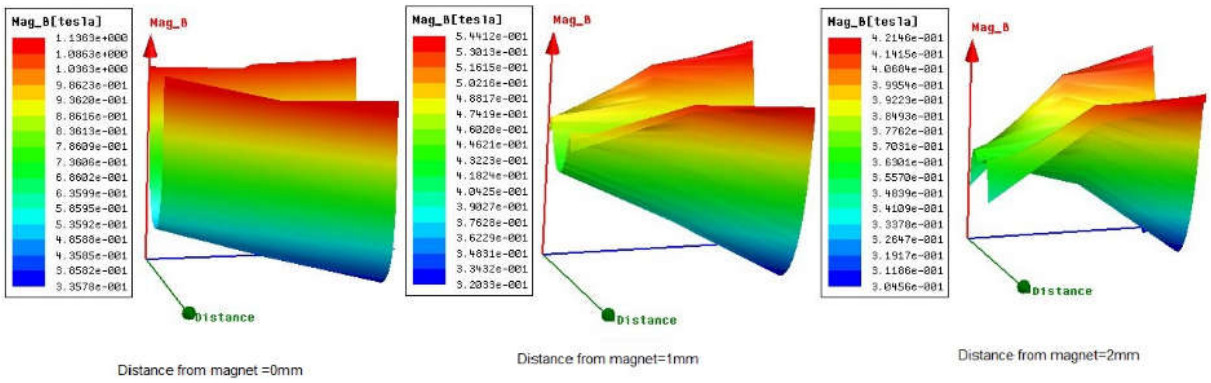

Figure 12. (color onlin) Magnetic flux density in the magnet of 20 mm height, with different diameters and different distances from the magnet surface.

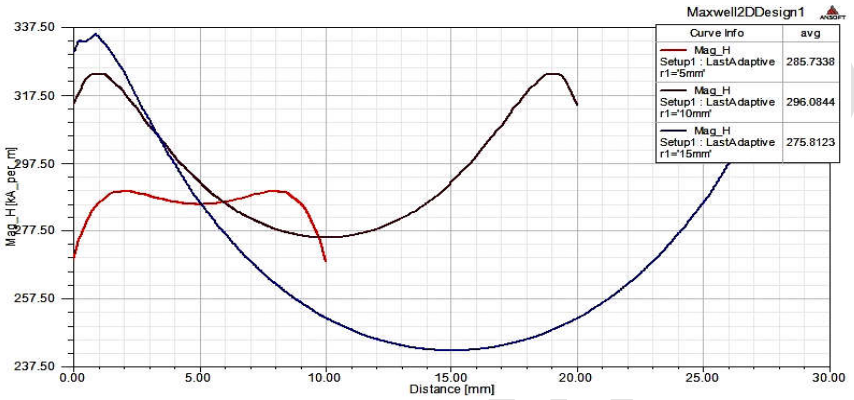

Figure 13. (color onlin) Magnetic field strength distribution in the N35 permanent magnet with different diameters and the height of 20 mm in a 2 mm distance from the magnet surface.

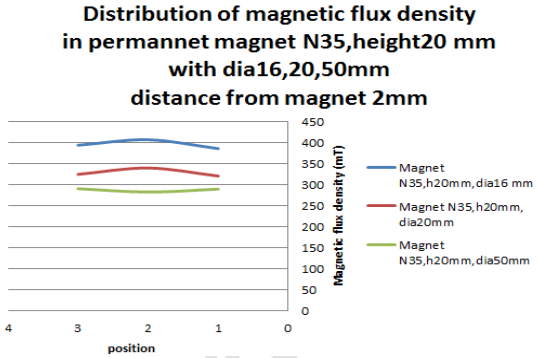

Figure 14. (color onlin) Measured values for magnetic flux density in the magnets with the constant height and the variable diameter.

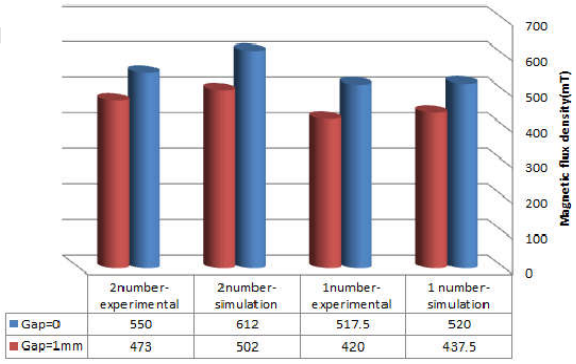

Figure 15. (color onlin) Measured and simulated values of one and two magnets in the surface and in a 1 mm distance from the surface.

Generally, cylindrical magnet can be classified in terms of the geometric structure. These are disk magnets (magnets whose diameter is higher than their height) or cylindrical magnets, whose height is higher than their diameter. According to the measured and simulated values, it can be concluded that using the cylindrical magnet, due to its uniform magnet flux density, can yield more desirable results in the MAF processes.

In figure 14, the measured values for the magnetic flux density in the magnets of 20 mm height and diameters of 16, 20 and 25 mm and at a 2 mm distance from the magnet surface are reported. As in the previous section, the measured and simulated values were correlated well with each other.

The maximum mean value for the magnet occurred when diameter was in the range of 15-20 mm and its height was 0 mm. As can be seen, decreasing the diameter resulted in lower flux density.

Sometimes, in order to increase the field intensity, magnets are attached to each other from the opposite poles. In figures 15, the results of simulation and measurement of this process are mentioned. As can be observed, attaching magnets does not multiply the field strength. Figure 15 also depicts the measured and

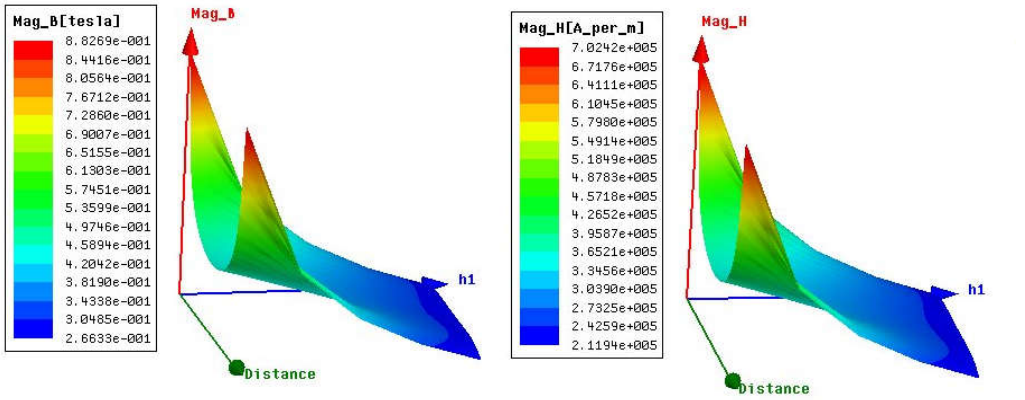

Figure 16. (color onlin) Magnetic flux density and field strength in a 16×20 mm magnet in different distances from the magnet.

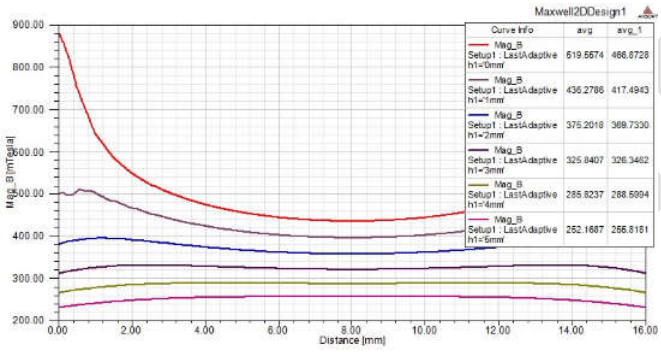

Figure 17. (color onlin) Magnetic field intensity distribution in different distances from the magnet.

simulated magnetic flux density of one and two magnets on the surface and at 1 mm distance from the magnet surface.

3. 3. Effect of gap

One of the important factors affecting magnetic field intensity is the finishing gap. In the process of MAF, the optimum quantity of gap is extremely important. In a fixed location of magnet, with an increase in the distance from the surface of the magnet, magnetic field intensity and magnetic flux density are reduced. If the gap between the surface of the work piece and the surface of magnet is extremely short in the process of magnetic abrasive finishing, the abrasive brush becomes rigid and leaves scratch on the surface of the work piece; if the gap becomes long, the magnet cannot retain magnetic abrasive powder at high rotational velocities. In figures 16 and 17, the effect of gap on the Nd35 magnet with the diameter of 16 mm and the height of 20 mm is shown. Certainly, it should be noted that in simulating the distance of gap, air with magnetic permeability (μ=1) is considered.

As can be seen from equation 3, field intensity complies with flux density based on $\vec{B} = \mu \vec{H}$. Of course, the harmony between these two is established only if the relation between flux density and magnetic field remains constant. In many materials, magnetic permeability coefficient varies in different field intensities (the relation between field strength and flux density is a curve and it is not a constant value). As can be seen from figure 16, by increasing the distance from the surface of the magnet, the curve behavior of the magnetic flux density is changed from concave to constant; then, it is changed, to some extent, to convex.

3. 4. Analysis of the effect of the work piece material, magnet holder and work piece fixture on the magnetic field strength

It is evident that magnet is placed in a fixture during the process of MAF. Work piece material as well as magnet fixture maeterial and work piece fixture are highly effective on the field intensity and the distribution of magnetic field intensity on the surface of the magnet. Aluminum with the magnetic permeability close to 1 is almost a non-ferromagnetic material, while steel is a ferromagnetic material. In experiments and simulation, these materials are used. The weight percentage of the ferromagnetic particles in the magnetic abrasive brush affects flux and magnetic field intensity, thereby influencing the finishing pressure and the magnetic force. It is important to note that the uniformity of the magnetic field intensity is critically important. If the difference between the surface center and its edges is remarkable, it can adversely affect the surface quality of the finished work piece.

Simulated model is shown in figure 18 with 2D and 3D modes. In the analysis carried out, the material parts considered are aluminum 7075 (non-ferromagnetic) and steel 1080 (ferromagnetic). In order to obtain effective parameters on the magnetic flux density, design of

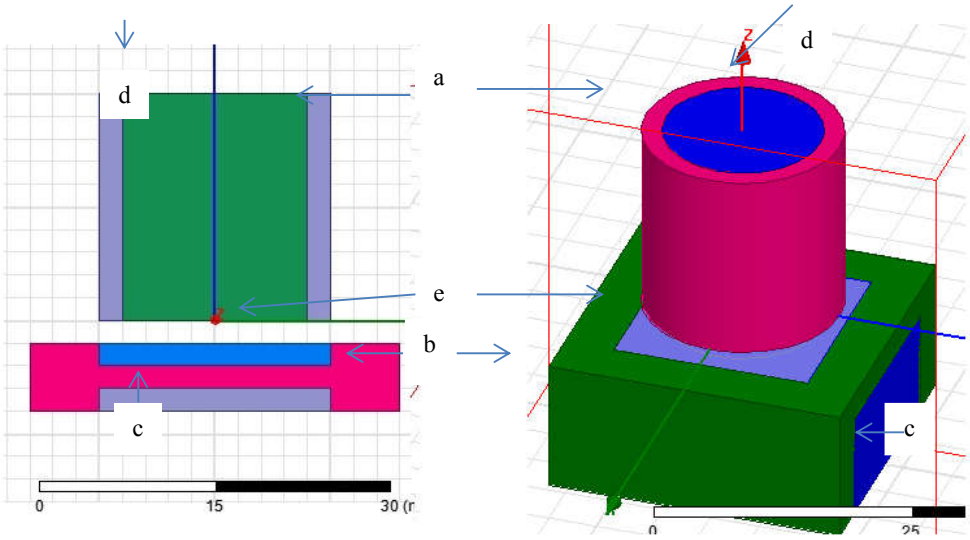

Figure 18. (color onlin) The used model in 2D and 3D simulations, (a) magnet fixture, (b) work piece fixture, (c) magnet, (d) magnet, and (e) work piece.

Table 4. Factors and levels.

Factor	Level	
Work piece	Al7075	Steel1080
Work piece fixture	Al7075	Steel1080
Magnet fixture	Al7075	Steel1080

Table 5. Simulation set up.

StdOrder	RunOrder	w.p	Wp-fixture	Magnet fixture	B(mT)-2mmgap
1	1	Al	Al	Al	0.37
2	2	steel	Al	Al	0.53
3	3	Al	steel	Al	0.504
4	4	steel	steel	Al	0.619
5	5	Al	Al	steel	0.378
6	6	steel	Al	steel	0.55
7	7	Al	steel	steel	0.488
8	8	steel	steel	steel	0.61

Table 6. Variance analysis of the output data.

Source	DF	Seq SS	Adj SS	Adj Ms	F	P
Main Effects	3	0.0597774	0.0597774	0.0199258	6376.25	0.009
Wp	1	0.0404701	0.0404701	0.0404701	12950.44	0.006
Fix-wp	1	0.0193061	0.0193061	0.0193061	6177.96	0.008
2-way Interactions	1	0.0000011	0.0000011	0.0000011	0.36	0.656
Wp*fix-wp	3	0.0015244	0.0015244	0.0005081	162.60	0.058
Wp*fix-magnet	1	0.0011281	0.0011281	0.0011281	361.00	0.033
Fix-wp*fix-magnet	1	0.0000451	0.0000451	0.0000451	14.44	0.164
Residual Error	1	0.0003511	0.0003511	0.0003511	112.36	0.060
total	1	0.0000031	0.0000031	0.0000031		
	7	0.0613049				

experiments as a statistical method is used. All simulation parameters and their chosen levels are presented in table 4. There are three factors and each factor has two chosen levels. There are eight setups for the simulation according to the full factorial design.
Magnetic flux density in 2 mm distance from magnet surface is response. Simulation setups with output values have been presented in the table 5. Effective factors and how they affect the value of magnetic flux density are obtained with variance analyses (ANOVA).

The corresponding values for ANOVA analysis have been presented in table 6. Statistical analysis and the governing mathematical equation have been derived by the MINITAB software. It should be noted that variables whose p value with the reliability of 95% are less than 5% are considered effective. As can be seen from the table, by considering (α=0.05), the work piece, magnet fixture and the interaction between the work piece and the work piece fixture are the effective factors.

Considering values of R-sq=99/96% and R-sq(adj)=99/67%, it can be said the proposed model complies appropriately with the data. Also, the plots for the main effects and their interaction are provided in figure 19.

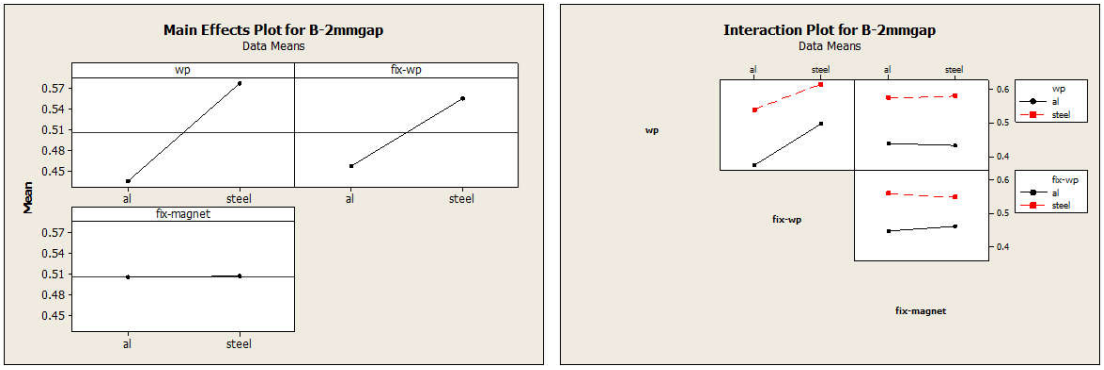

Figure 19. (color onlin) Main effect plot and the interaction plot for magnetic flux density (gap=2mm).

(a) (b)

Figure 20. (color onlin) Magnetic flux density measurement. a) all parts are non-ferromagnetic, b) work piece fixture and magnet are ferromagnetic, while the work piece is non-ferromagnetic.

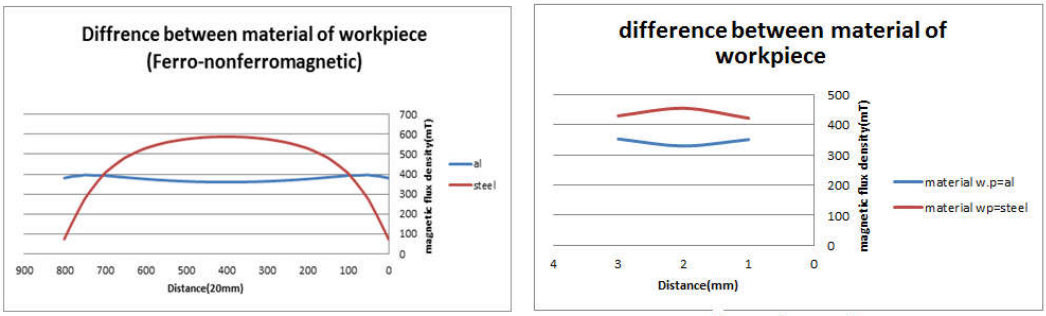

(simulation) (experimental)

Figure 21. (color onlin) Simulation and measurement of the effect of work piece material on the magnetic flux density.

It can be inferred from figures 19 that variation in the material of work piece and work piece fixture can affect magnetic flux density, while the magnet fixture material is not effective. Furthermore, interaction of the parameters reveals that in a ferromagnetic work piece, a ferromagnetic work piece fixture increases the magnetic flux density. However, if work piece is non-ferromagnetic, the influence of a ferromagnetic fixture is more remarkable. Moreover, when work piece fixture is ferromagnetic, a non-ferromagnetic magnet fixture boosts the magnetic flux density imposing on the work piece surface.

Based on the obtained results from simulations, the regression model was obtained for predicting the magnetic flux density according to equation (19). Magnetic flux density value is considered as a dependent variable, and work piece material, fixture material, and magnet fixture are considered as the independent ones.

$$B(T) = 0.506 + 0.07 \times W.P + 0.04 \times W.P\,\text{fixture} - 0.011 \times W.P \times W.P\,\text{fixture} \quad (19)$$

Magnetic flux density measurement in different conditions has been shown in figure 20. In figure 20-a, work piece fixture, magnet fixture and also work piece are non-ferromagnetic. In figure 20-b, magnet fixture and work piece fixture are ferromagnetic and work piece is non-ferromagnetic.

In figure 21, the trend of changes in magnetic flux density in aluminum and steel work piece for measurements and simulation are shown. The material of the work piece fixture and magnet fixture is non-ferromagnetic aluminum. The difference in the behavior toward work pieces with different materials (ferromagnetic and non-ferromagnetic) and the difference in the mean of quantities are distinct. In the results obtained by the performed measurements with similar conditions, this difference is confirmed.

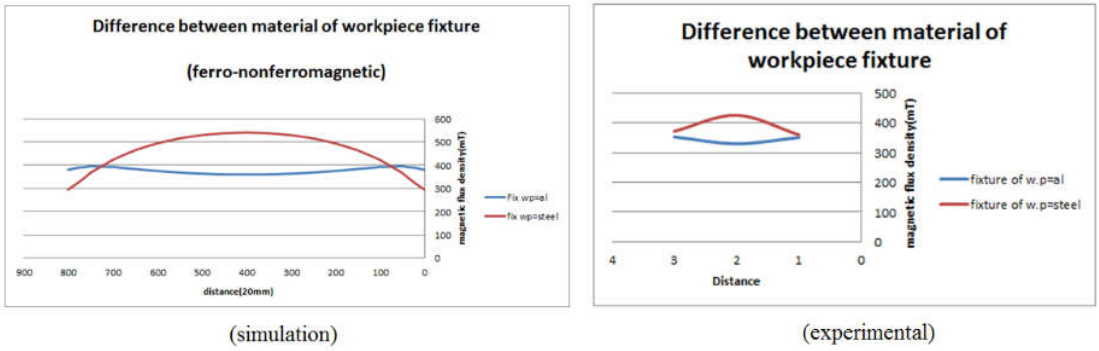

Figure 22. (color onlin) Simulation and measurement of the effect of fixture material on the magnetic flux density.

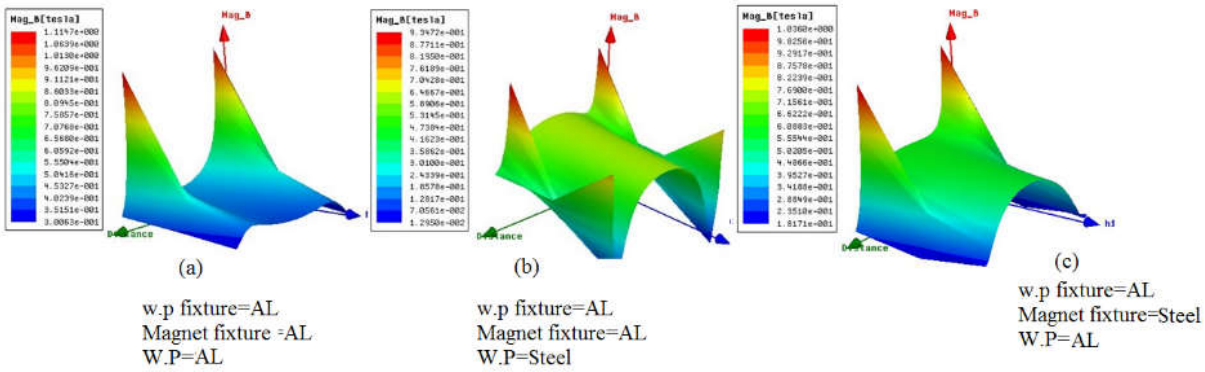

Figure 23. (color onlin) Magnetic flux density plot in 2 mm distance from the magnet surface.

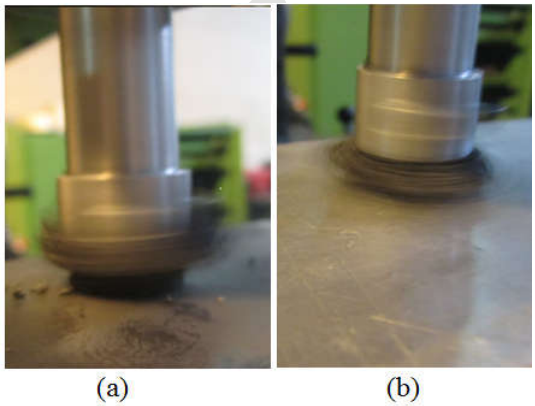

Figure 24. (color onlin) (a) Iron work piece, and (b) Aluminum work piece.

Furthermore, the effect of using iron work piece fixture is shown in the figure 22. The reason for this difference is in making a closed loop of magnet with ferromagnetic parts. In other words, ferromagnetic parts act like an opposite pole against the magnet. The material of the work piece and magnet fixture is non-ferromagnetic.

Moreover, concavity and convexity directions of the curve against parts with different qualities can be observed in figures 22 and 23. In ferromagnetic parts, the magnetic flux density is higher in the center area of the surface in comparison with the edges; in contrast, for non-ferromagnetic parts, edges undergo higher magnetic flux density than the center area of the surface. Moreover, the magnetic flux density for ferromagnetic materials is higher than that for non-ferromagnetic ones. The maximum and minimum magnetic flux density is given by the cubic plot (figure 23). In figure 23 (a), all of the parts are non-ferromagnetic and in figure 23 (b), work piece is ferromagnetic and in figure 23-c, the magnet fixture is ferromagnetic, and others are non-ferromagnetic. To confirm this issue, the formation of abrasive bush is also shown in figure 24. The closed angle and concentration of powders can be seen in the iron work pieces .

As can be seen, the effect of a ferromagnetic work piece is similar to that of a ferromagnetic work piece fixture. In the finishing of non-ferromagnetic materials, one method to increase magnetic flux density and

(a) (b)

Figure 25. (color onlin) (a) Non-ferromagnetic magnet fixture, and (b) ferromagnetic magnet fixture.

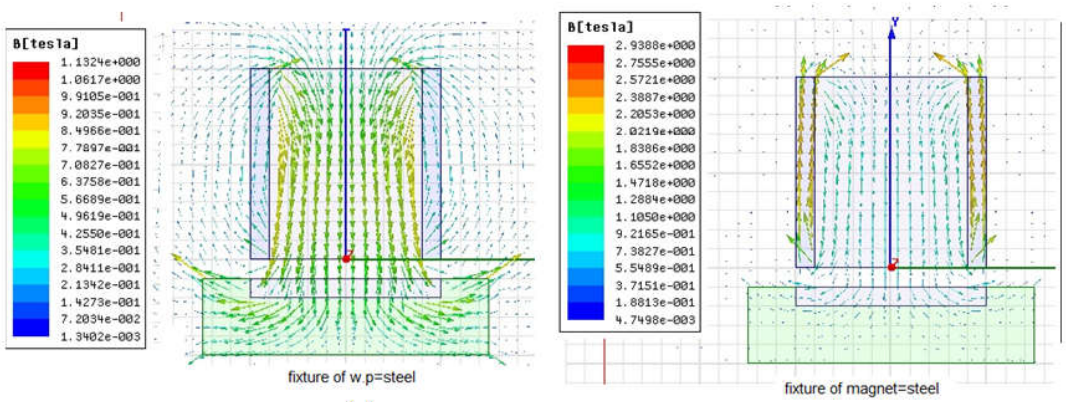

Figure 26. (color onlin) Establishment of the closed ring, (a) ferromagnetic work piece fixture, and (b) ferromagnetic magnet fixture.

produce a close circuit is to use the ferromagnetic work piece fixture. However, the increase in the magnetic flux density in the center area of the surface can lead to the scratching of the surface due to the higher cutting velocity in the center. Introducing grooves in the magnet by the use of ring shape magnets is considered as a precaution for this problem.

To confirm this, the development of the abrasive brush is illustrated in figure 24. A tight angle and a high concentration of the powder can be observed in iron work pieces and work piece fixtures. In figure 24 (a), the work piece is made of iron and in figure 24 (b), it is made of aluminum. The pattern of the powder concentration on the iron work piece surface and powder distribution on the aluminum work piece surface, while rotating, can be seen in this figure.

In figure 25, the formation of magnetic chains can be seen easily. The used powder is steel particle with the size of 1 mm. To see the formation of magnetic abrasive bush better, relatively large particles are used.

Magnet fixture made from aluminum and steel can be seen in the figure 25. The formation of abrasive powder is very clear in the figure. As can be seen from the figure, for iron work piece fixture, some powder is absorbed in the edges of the fixture, leading to the better efficiency of MAF for non-ferromagnetic materials, but it is not suitable for the polishing of the ferromagnetic parts. In aluminum work piece, the fixture powder does not adhere to the lower edges of the fixture. It is worth noticing that this is not the case for the side edges of the fixture, where powder can easily adhere to the body of the aluminum fixture while such a thing cannot be observed for the iron fixture. As mentioned, the body of the iron fixture acts as the return lines of the magnetic field and a close circuit is produced between the magnet and the fixture. This is not the case for aluminum fixture.

Establishment of closed ring can be seen in the figure 26. In figure 26 (a) work piece fixture is ferromagnetic and in 26 (b), the magnet fixture is ferromagnetic. Other parts are non-ferromagnetic.

4. Conclusion

In the permanent magnet with a constant diameter, an increase in height leads to enhancing the magnetic flux density and the magnetic field intensity.

In a permanent magnet with a constant height, an increase in diameter leads to a decrease in the magnetic flux density and an increase in the variation of the magnetic density on the magnet surface.

By placing a magnet on the top of another magnet (cylindrical with the diameter of 16 mm and the height of 20mm), the magnetic flow density at 1 mm distance from the magnet surface was increased by 15% and 13% in the simulation and measurements, respectively.

Increasing the distance from the magnet surface resulted in a decrease in the magnetic flux density and showed the significance of the edge phenomenon effect.

The amount of the applied force on the abrasive particle (with the diameter of 10 micron) in the cylindrical magnet at 2 mm distance from the magnet

surface was 2.3×10^{-7} N, and the penetration depth in the surface was 4×10^{-8} m.

The effects of work piece material, work piece fixture material, and the interaction of them were significant on the magnetic flux density.

To concentrate the magnetic abrasive powder in the polishing process of non-ferromagnetic parts, the ferromagnetic fixture for these parts could be provided. Material for magnet fixture did not affect the magnetic flux density significantly, but it is recommended to use the ferromagnetic material for the MAF process efficiency.

References

1. V Jain, *Journal of Materials Processing Technology* **209**, 20 (2009) 6022.
2. N Jain, V Jain, and S Jha, *The International Journal of Advanced Manufacturing Technology* **34**, 11-12 (2007) 1191.
3. S Jha and V Jain, "*Nanofinishing Techniques*, *in: Micromanufacturing and Nanotechnology*", Eds. Springer (2006) 171.
4. V Ganguly, T Schmitz, A Graziano, and H Yamaguchi, Force Measurement and Analysis for Magnetic Field–Assisted Finishing, *Journal of Manufacturing Science and Engineering* **135**, 4 (2013) 041016.
5. Y M Hamad, *Al-Khwarizmi Engineering Journal* **6**, 4 (2010) 10.
6. R S Mulik and P M Pandey, *Journal of Manufacturing Science and Engineering* **134**, 5 (2012) 051008.
7. S Jayswal, V Jain, and P Dixit, *The International Journal of Advanced Manufacturing Technology* **26**, 5-6 (2005) 477.
8. D K Singh, V Jain, and V Raghuram, *Journal of Materials Processing Technology* **149**, 1 (2004) 22.
9. D K Singh, V Jain, and V Raghuram, *The International Journal of Advanced Manufacturing Technology*, **30**, 7-8 (2006) 652.
10. V Mishra, H Goel, R S Mulik, and P Pandey, *Journal of Manufacturing Processes* **16**, 2 (2014) 248.
11. L D Yang, C T Lin, and H M Chow, *The International Journal of Advanced Manufacturing Technology* **42**, 5-6 (2009) 595.
12. J S Kwak and H S Kang, "*Assessment on Magnetic Flux Density of Magnetic Array Table in Magnetic Abrasive Polishing Process*", Proceeding of the International Multi-Conference of Engineering and Computer Scientists (IMECS), Hong Kong, Vol. II, (2011).
13. J S Kwak, *Journal of Machine Tools and Manufacture* **49**, 7 (2009) 613.